**Supplementary Information (SI)**

# Dependence of particle nucleation and growth on high molecular weight gas phase products during ozonolysis of α-pinene

J. Zhao[1,2], J. Ortega[2], M. Chen[1], P. H. McMurry[1], and J. N. Smith[2,3]

[1]Department of Mechanical Engineering, University of Minnesota, Minneapolis, Minnesota, 55455, USA

[2]Atmospheric Chemistry Division, National Center for Atmospheric Research, Boulder, Colorado, 80307, USA

[3]Department of Applied Physics, University of Eastern Finland, Kuopio 70211, Finland

The supplementary material contains three sections.

**Section I:** contains 3 tables and 6 figures.

Table S1. Summary of experimental conditions in this study.

| Exp. | α-pinene | Ozone | | Cluster CIMS reagent ions |
|---|---|---|---|---|
| | (ppb) | first 3 hours (ppb $min^{-1}$) | steady state (ppb) | |
| **E1** | 20 | 0.2 | 75 | Nitrate dimer |
| **E2** | 5 | 0.1 | 50 | Nitrate dimer |
| **E3** | 20 | N/A | 75 | Acetate dimer |

Table S2. Summary of all measured Category II products for *E1*: ion (m/z), peak concentration (in $cm^{-3}$), corresponding neutral identities, and correlation coefficients with > 20 nm particles.

| Ion (m/z) | Peak conc.[a] ($cm^{-3}$) | $NO_3^-$ Clusters?[b] | Corresponding neutral[b] | | Correlation coefficient[c] |
|---|---|---|---|---|---|
| | | | Mass (amu) | Formula | |
| 142 | $2.5x10^5$ | | | | 0.63 |
| 158 | $2.1x10^5$ | | | | 0.67 |
| 228 | $3.0x10^5$ | | | | 0.66 |
| 240 | $4.2x10^6$ | Y | 178 | $C_5H_6O_7$ | 0.80 |
| 241 | $3.9x10^5$ | | | | 0.60 |
| 257 | $2.6x10^5$ | | | | 0.75 |
| 282 | $8.9x10^5$ | Y | 220 | $C_7H_8O_8$ or $C_8H_{12}O_7$ | 0.51 |
| 287 | $5.2x10^5$ | | | | 0.82 |
| 297 | $5.3x10^5$ | | | | 0.81 |
| 298 | $4.3x10^5$ | Y | 236 | $C_8H_{12}O_8$ | 0.69 |
| 308 | $2.6x10^6$ | Y | 246 | $C_{10}H_{14}O_7$ | 0.78 |
| 309 | $5.2x10^5$ | | | | 0.66 |
| 310 | $1.1x10^6$ | Y | 248 | $C_9H_{12}O_8$ or $C_{10}H_{16}O_7$ | 0.77 |
| 326 | $7.5x10^5$ | | | $C_9H_{12}O_9$ or $C_{10}H_{16}O_8$ | 0.61 |
| 327 | $5.5x10^5$ | | | | 0.80 |
| 329 | $2.5x10^5$ | | | | 0.82 |
| 339 | $8.0x10^5$ | | | | 0.72 |
| 341 | $4.6x10^5$ | | | | 0.61 |
| 343 | $3.0x10^5$ | | | | 0.50 |
| 355 | $5.5x10^5$ | | | | 0.74 |
| 356 | $4.3x10^5$ | Y | 294 | $C_{10}H_{14}O_{10}$ | 0.61 |
| 371 | $3.1x10^5$ | | | | 0.53 |
| 375 | $2.0x10^5$ | | | | 0.57 |

[a] Concentration: background subtracted peak concentration (in $cm^{-3}$) at time c in Fig. 1b;

[b] from Ehn et al. 2011;

[c] Correlation was performed with the concentration of >20 nm particles for time period t=0-10 hr in Fig. 1b (t=0 was defined as the time when ozone was added to the chamber).

1 Table S3. Summary of all measured m/z of category III products for *E1*.

| Ion (m/z) |
|---|
| 152, 154, 160, 164, 165, 166, 167, 168, 178, 179, 180, 182, 183, 192, 194, 196, 198, 206, 208, 209, 210, 212, 213, 214, 217, 218, 220, 222, 223, 224, 225, 226, 227, 234, 235, 236, 238, 239, 244, 246, 248, 249, 250, 251, 252, 253, 254, 262, 264, 265, 266, 267, 268, 270, 277, 278, 279, 280, 281, 285, 292, 293, 294, 295, 296, 307, 311, 313, 314, 324, 325 ,357 |

2

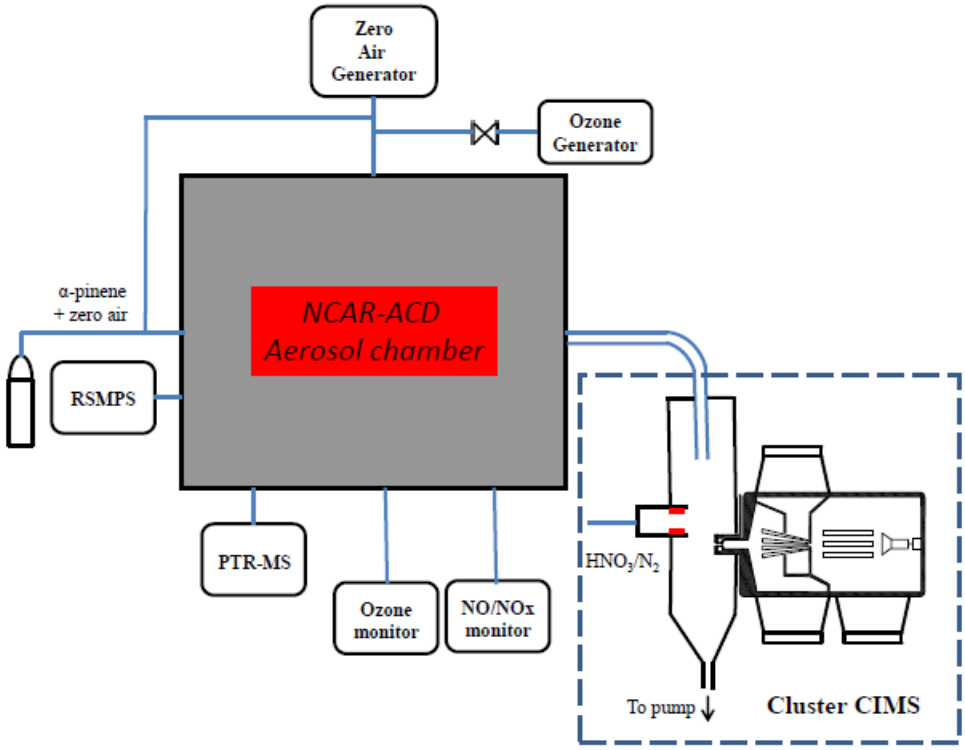


Fig. S1. Schematic diagram of the NCAR reaction chamber and the instruments used in this study.

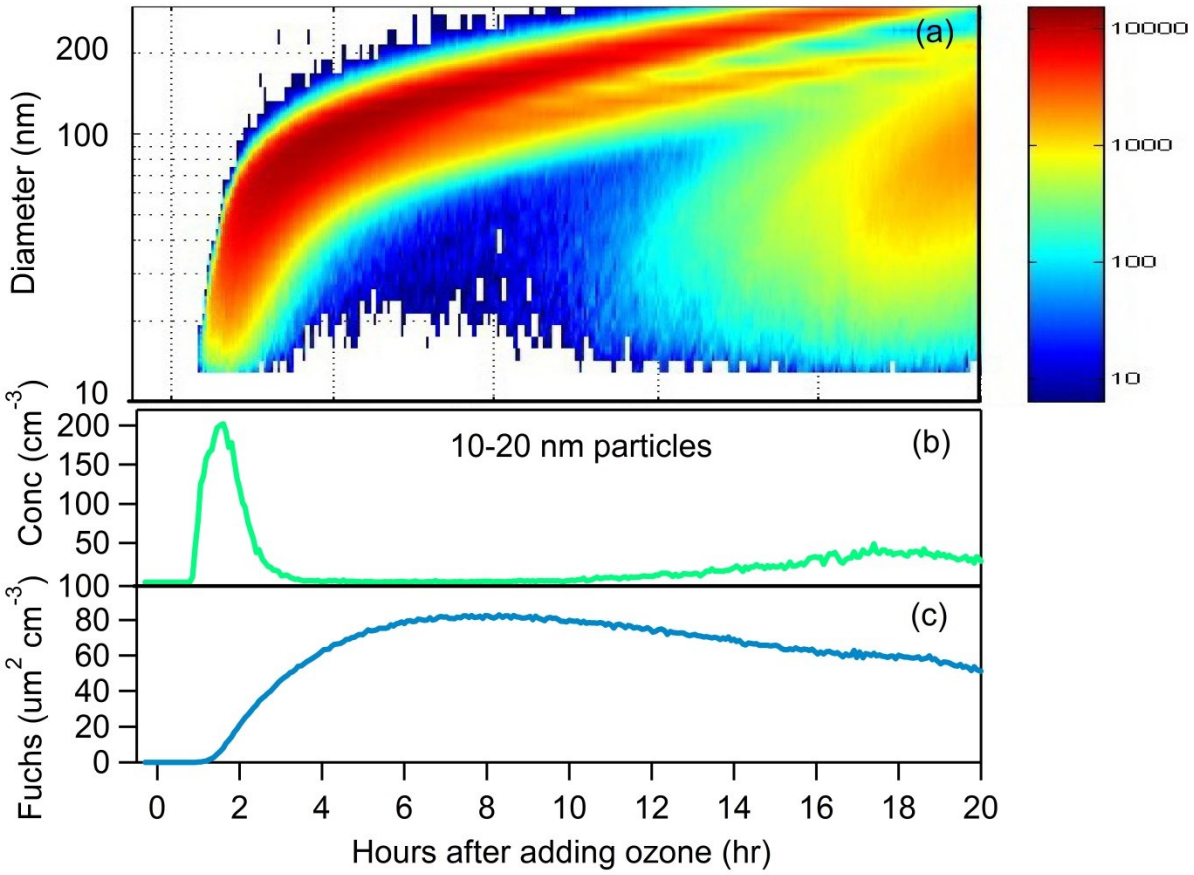


Fig. S2. Characteristics of particle formation from chamber α-pinene ozonolysis for *E2*: (a) Contour plot of the particle size distribution measured with the SMPS in the 10-350 nm diameter range; (b) Temporal total concentration of 10-20 nm particles; (c) Estimated time-dependent Fuchs surface area (in $\mu m^2\ cm^{-3}$).

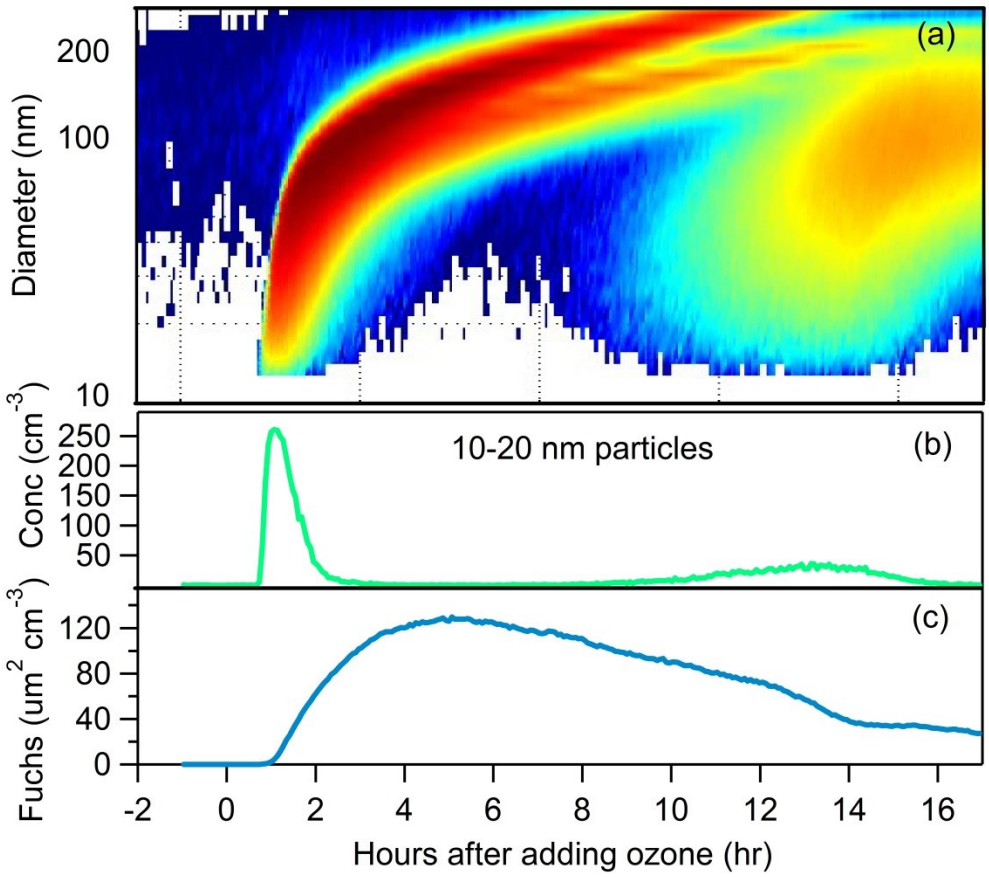


Fig. S3. Characteristics of particle formation from chamber α-pinene ozonolysis for *E3*: (a) Contour plot of the particle size distribution measured with the SMPS in the 10-350 nm diameter range; (b) Temporal total concentration of particles between 10 and 20 nm; (c) Estimated time-dependent Fuchs surface area (in $\mu m^2\ cm^{-3}$).

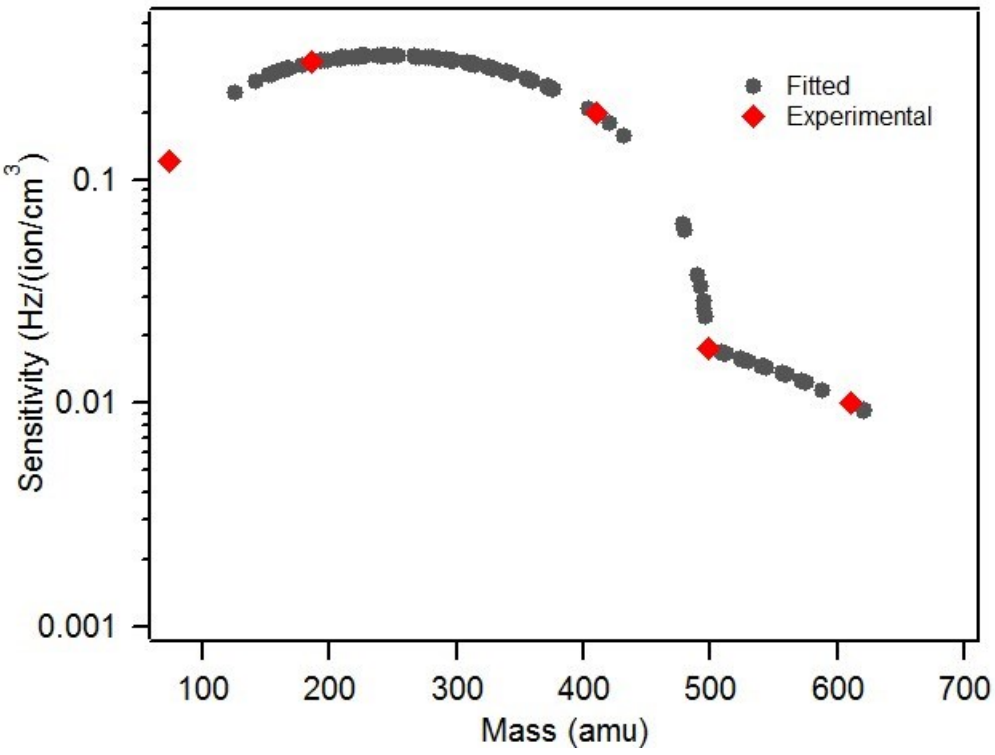


Fig. S4. Mass-dependent sensitivities used for estimating concentrations of oxidation products (Zhao et al., 2010).

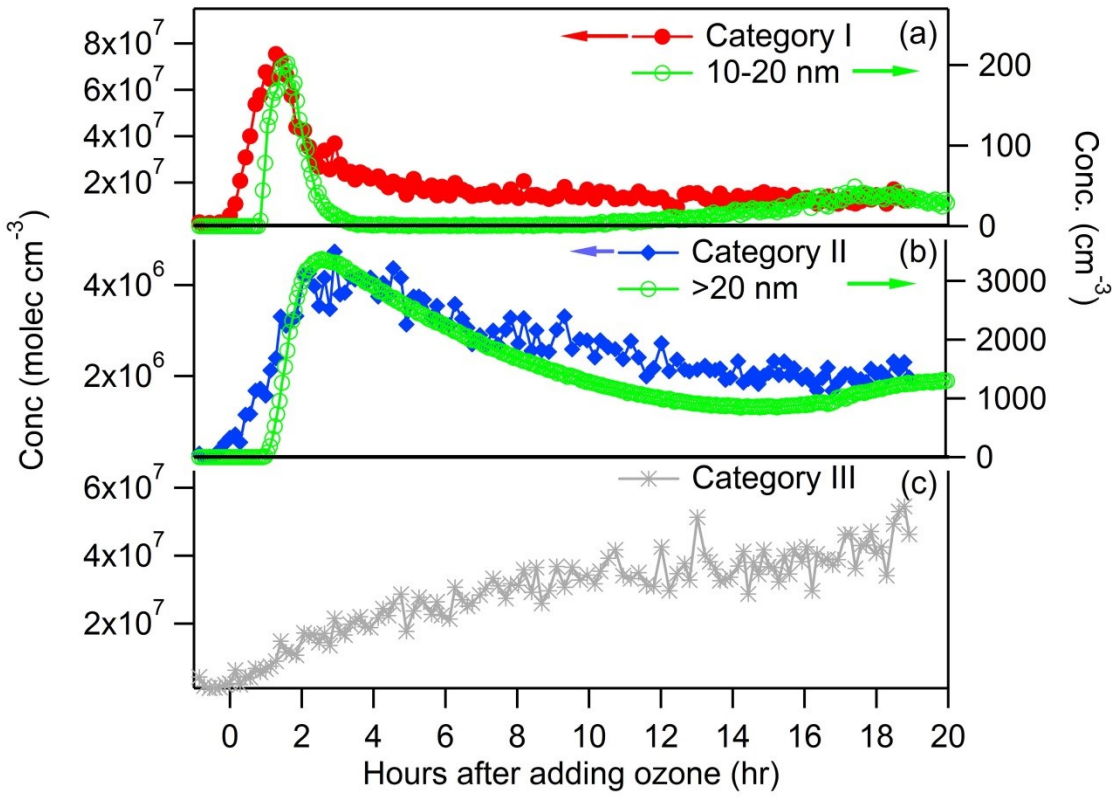


Fig. S5. Time-dependent total concentrations of the category I-III products measured with the Cluster CIMS, along with the total concentrations of 10-20 nm particles and particles larger than 20 nm measured with the SMPS for *E2*. (a) Category I products and 10-20 nm particles; (b) Category II products and particles larger than 20 nm; (c) Category III.

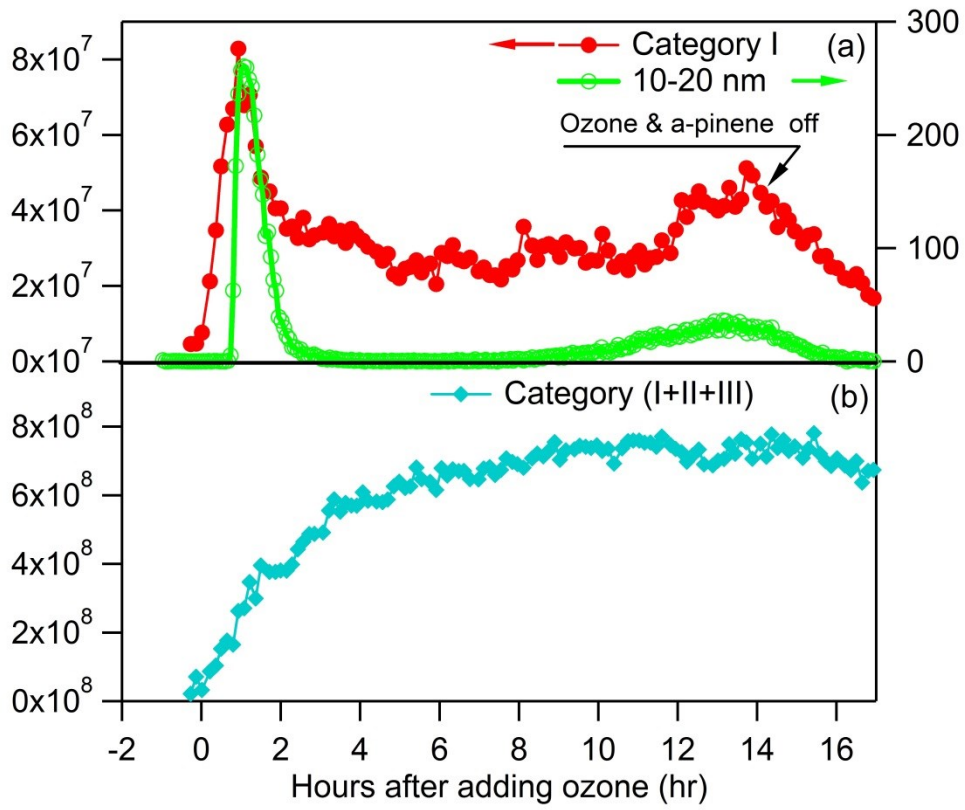


Fig. S6. Time-dependent total concentrations of the category I-III products measured with the Cluster CIMS, along with the total concentrations of 10-20 nm particles measured with the SMPS for *E3*. (a) Category I products and 10-20 nm particles; (b) Category (I+II+III) products.

**Section II:** This section describes the method used to estimate the formation and growth rates of the first and second events for *E1-E3*.

1. Method:

The evolution of particle concentrations between 10 nm and 20 nm can be estimated from the following general dynamic equation (eq. 1) (Gelbard and Seinfeld, 1974).

$$\frac{dN_{10-20}}{dt} = J_{10nm} - J_{20nm} + CoagSrc - CoagSnk \qquad (1)$$

$\frac{dN_{10-20}}{dt}$ is the rate of change of particle concentrations between 10 and 20 nm. For *E1-E3*, this rate was assumed to increase was linearly with time during the first half an hour when nucleation occurs. Thus it can be approximated as $\frac{\Delta N_{10-20}}{\Delta t}$, the concentration change divided by the time (half an hour). $J_{20nm}$ is the formation rate of particles at 20 nm, which can be expressed as $\left.\frac{dN}{dDp}\right|_{20nm} \cdot GR$.

GR is the modal growth rate at 20 nm, and is estimated with the method described by Stolzenburg (2005). *CoagSrc* and *CoagSnk* are the coagulation source and coagulation sink terms respectively. These two terms are calculated according to Kuang et al. (2012).

Rearranging eq. 1, the particle formation rate at 10 nm ($J_{10nm}$) can then be calculated by eq. 2.

$$J_{10nm} \approx \frac{\Delta N_{10-20}}{\Delta t} + \left.\frac{dN}{dDp}\right|_{20nm} \cdot GR - CoagSrc + CoagSnk \qquad (2)$$

2. Summary of particle formation rates and growth rates for *E1-E3*.

Table S4. Summary of formation rates and growth rates for *E1-E3*

| Exp. | 1st event | | 2nd event | |
|---|---|---|---|---|
| | Form. Rate ($cm^{-3}$ $sec^{-1}$) | Growth Rate (nm $hr^{-1}$) | Form. Rate ($cm^{-3}$ $sec^{-1}$) | Growth Rate (nm $hr^{-1}$) |
| **E1** | 0.42 | 36 | 0.038 | 28 |
| **E2** | 0.28 | 16 | 0.026 | 12 |
| **E3** | 0.53 | 23 | 0.022 | 13 |

**Section III:** This section describes how to estimate the minimum concentrations for growth of particles at the measured growth rates for *E1-E3.*

The minimum concentration of a monomer N1 required to grow particles at a certain rate can be estimated by eq. 3. (Kuang et al., 2010).

$$GR = \frac{1}{2} v_1 N_1 \bar{c} \qquad (3)$$

Where GR is the diameter growth rate, $v_1$ is the molecular volume for monomer and $\bar{c}$ is the thermal velocity of the monomer. A molecular weight of 500 amu is assumed for Category I products.

Table S5. Summary of minimum concentrations of a low molecular weight vapor (i.e. N1=$N_{98amu}$) or a high molecular weight vapor (i.e. N1=$N_{500amu}$) required to grow particle at the observed growth rates for *E1-E3*

| Exp. | 1st event | | 2nd event | |
|---|---|---|---|---|
| | $N_{98amu}$ ($cm^{-3}$) | $N_{500amu}$ ($cm^{-3}$) | $N_{98amu}$ ($cm^{-3}$) | $N_{500amu}$ ($cm^{-3}$) |
| **E1** | $8.3x10^8$ | $3.3 x10^8$ | $6.5 x10^8$ | $2.5x10^8$ |
| **E2** | $3.7 x10^8$ | $1.4 x10^8$ | $2.8 x10^8$ | $1.1x10^8$ |
| **E3** | $5.3 x10^8$ | $2.1 x10^8$ | $3.0 x10^8$ | $1.2x10^8$ |

References:

Gelbard, F., Seinfeld J. H.: Numerical-Solution of Dynamic Equation for Particulate Systems, J. Comput. Phys., 28, 357-375, 1978.

Kuang, C., Riipinen, I., Sihto, S. L., Kulmala, M., McCormick, A. V., McMurry, P. H.: An improved criterion for new particle formation in diverse atmospheric environments, Atmos. Chem. Phys., 10, 8469-8480, 2010.

Kuang, C., Chen, M., Zhao, J., Smith, J., McMurry, P. H., and Wang J.: Size and time resolved growth rate measurements of 1 to 5 nm freshly formed atmospheric nuclei, Atmos. Chem. Phys., 12, 3573-3589,2012.

Stolzenburg, M. R., McMurry, P. H., Sakurai, H., Smith, J. N., Mauldin, R. L., Eisele, F. L., Clement, C. F.: Growth rates of freshly nucleated atmospheric particles in Atlanta, J. Geophys. Res., 110, D22S05, doi:10.1029/2005JD005935, 2005.

Zhao, J., Eisele, F. L., Titcombe, M., Kuang, C. G., and McMurry, P. H.: Chemical ionization mass spectrometric measurements of atmospheric neutral clusters using the cluster-CIMS, J. Geophys. Res., 115, D08205, doi:10.1029/2009JD012606, 2010.